



Design specifications of direct borohydride–hydrogen peroxide fuel cell system for space missions



Taek Hyun Oh*

Launcher Thermal & Aerodynamics Team, Launcher Technology Development Office, KSLV-II R&D Head Office, Korea Aerospace Research Institute (KARI), 169-84 Gwahak-ro, Yuseong-gu, Daejeon 34133, Republic of Korea

ARTICLE INFO

Article history:

Received 29 February 2016

Received in revised form 11 September 2016

Accepted 12 September 2016

Available online 19 September 2016

Keywords:

Sodium borohydride

Hydrogen peroxide

Direct borohydride–hydrogen peroxide fuel cell

Design specification

Space mission

ABSTRACT

The design specifications of a direct borohydride–hydrogen peroxide fuel cell (DBPFC) system for space missions were determined based on the energy density. A unit cell test of the DBPFC with electrocatalysts supported on multiwalled carbon nanotubes was conducted to evaluate the DBPFC performance. A relationship between the current density and voltage was obtained from the test results to estimate the total mass and energy density of the DBPFC system. The effects of changing the voltage efficiency and fuel concentrations on the total mass of the DBPFC system were investigated to determine the appropriate design specifications for space missions. When the voltage efficiency was 35%, the system mass was the lowest, regardless of the fuel concentrations. Finally, the energy density of the DBPFC system operating at the optimum voltage efficiency was calculated at various fuel concentrations. When the NaBH₄ and H₂O₂ concentrations are higher than 20 and 65 wt%, respectively, the energy density (>400 Wh/kg) of the DBPFC system is higher than those of other power sources and the DBPFC system can be widely used for space missions.

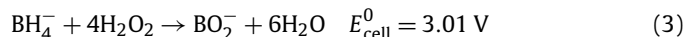
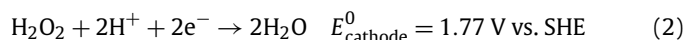
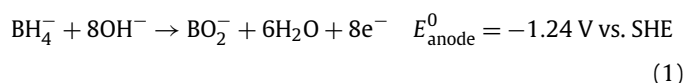
© 2016 Elsevier Masson SAS. All rights reserved.

1. Introduction

Proton exchange membrane fuel cells (PEMFCs) have been widely used as power sources for mobile applications [1–14] owing to their advantages such as high efficiency, high energy density, fast response characteristics, and low noise. However, PEMFCs are not suitable for space missions because of hydrogen storage problems. Although liquid hydrogen has high gravimetric and volumetric energy densities, boil-off problems limit the mission duration. Gaseous hydrogen and metal hydrides, on the other hand, have low gravimetric and volumetric energy densities.

In countries with advanced aerospace technology, various institutes (the Indian Institute of Science [15–21], University of Southampton [22,23], University of Illinois [24–29], Harbin Engineering University [30,31], Xiangtan University [32–42], Tsinghua University [43], Ohio State University [44,45], Instituto Superior Técnico [46–48], Nanjing University [49], University of Maryland [50,51], KAIST [52–56], and Taiyuan University of Technology [57–59]) have developed direct borohydride–hydrogen peroxide fuel cells (DBPFCs) to solve the problems associated with PEMFCs. DBPFCs use liquid fuels instead of gaseous fuels. Elec-

tricity is generated by direct electrochemical reactions of sodium borohydride (NaBH₄) and hydrogen peroxide (H₂O₂) solutions, as shown in Eqs. (1)–(3).



DBPFCs can be used for space missions owing to their advantages. For example, solar cells can only be used in an environment with sunlight, but DBPFCs can be used in any environment. Batteries have low gravimetric energy density, but DBPFCs have high gravimetric energy density. Atomic batteries have some safety issues, but DBPFCs use liquid fuels that are environmentally friendly. Furthermore, DBPFCs are simple systems that have high theoretical voltage, high maximum power density, fast response characteristics, easy cooling, easy refueling, and easy fuel storage. In addition, fuel storage systems for fuel cell and propulsion systems can be integrated because H₂O₂ is widely used for space propulsion such as in monopropellant thrusters [60–63], bipropellant thrusters [64–66], and hybrid rockets [67].

However, the performance of the DBPFCs is still inferior to that of PEMFCs because of fuel decomposition, fuel crossover, and de-

* Fax: +82 42 860 2697.

E-mail address: thoh@kari.re.kr.

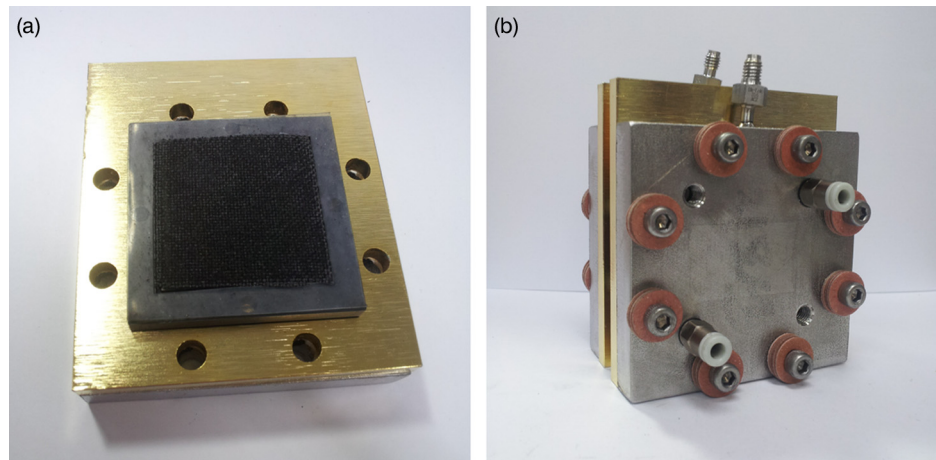


Fig. 1. Unit cell for fuel cell test: (a) components and (b) unit cell.

position of the reaction product on the electrocatalysts [52]. The performance of DBPFCs should be further improved to compete with other power sources for space missions. Research on the electrocatalysts, bipolar plates, fuel cell stack, and DBPFC system has been conducted by many research groups, but the design specifications of the DBPFC system have rarely been investigated.

Because a higher energy density of the power sources implies better mission capability, energy density is an important performance parameter for space missions. As a result, the design specifications of the DPBFC system for space missions were determined based on the energy density. First, the performance of a DBPFC with electrocatalysts supported on multiwalled carbon nanotubes (MWCNTs) was evaluated to obtain a relationship between current density and voltage. Second, the total mass of the DBPFC system was calculated at various voltage efficiencies and fuel concentrations to investigate the effect of those parameters on the system mass. Finally, the energy density of a DBPFC system operating at the optimum voltage efficiency was estimated at various fuel concentrations. The design specifications of the DPBFC system were determined, and the energy density of the DBPFC system was compared with other power sources.

2. Experimental

2.1. Electrode preparation

MWCNTs (Carbon Nano-material Technology, Korea) were heated at 400 °C for 4 h to remove impurities. Electrocatalysts were supported on MWCNTs using our previous procedure [53]. Each catalyst solution for the anode and cathode catalysts was prepared with a metal salt and sodium citrate ($C_6H_5Na_3O_7$, Junsei Chemical, Japan). The metal salts for the anode and cathode catalysts were palladium chloride ($PdCl_2$, Alfa Aesar, USA) and gold chloride ($AuCl_3$, Alfa Aesar, USA), respectively. Sodium citrate was used to disperse the catalyst. The MWCNTs were immersed in the catalyst solution, and then agitated in an ultrasonic bath (JAC-1505, Kodo Technical Research, Korea) for 30 min. The catalyst was reduced on the MWCNTs using 20 mL of $NaBH_4$ (Samchun Chemical, Korea) solution. A syringe pump (KDS 100, KD Scientific, USA) supplied the $NaBH_4$ solution to the catalyst solution for 1 h, after which it was agitated with a magnetic stirrer at 100 rpm for 5 h. The electrocatalyst supported on MWCNTs was washed with distilled water (H_2O , OCI, Korea) and dried at 100 °C for 2 h in a convection oven.

Each electrode (anode and cathode) was manufactured using a catalyst slurry and carbon cloth [53]. The catalyst slurry was

composed of the catalyst, 5 wt% Nafion solution (D521, DuPont, USA), and methanol (CH_3OH , OCI, Korea) (catalyst:Nafion solution:methanol = 1:1:20). The slurry was dispersed in an ultrasonic bath for 30 min, after which it was coated on carbon cloth (Fuel Cell Earth, USA). The piece of carbon cloth was 3.2 cm (width) \times 3.2 cm (length) \times 0.04 cm (thickness) and the catalyst loading for the carbon cloth was 1 mg/cm². The electrode was then dried by heating in a convection oven at 80 °C for 20 min. The dried electrode was immersed in a sulfuric acid solution (H_2SO_4 , Samchun Chemical, Korea) for 30 s. Finally, the electrode was washed with copious amounts of H_2O and dried at 80 °C for 1 h in a convection oven.

2.2. Electrode characterization

The electrode was investigated by various analyses. Transmission electron microscopy (TEM, Tecnai F20, Philips, Netherlands) was used to analyze the catalyst distribution on MWCNTs. Scanning electron microscopy (SEM, Nova 230, FEI, USA) and energy dispersive spectroscopy (EDS, Nova 230, FEI, USA) were used to investigate the surface morphology and composition, respectively, of the electrode. X-ray diffraction (XRD, D/MAX-2500, RIGAKU, Japan) was used to determine the microstructure of the electrode.

2.3. Unit cell for fuel cell test

Fig. 1 shows a unit cell for the fuel cell test. The unit cell consists of a Nafion 212 membrane (DuPont, USA), two electrodes (anode and cathode), two silicon gaskets (thickness: 0.25 mm, Fuel Cell Earth, USA), two bipolar plates, two collectors, and two end plates. The membrane was cleaned to remove organic contaminants by immersing it in 200 g of a solution composed of 3 wt% H_2O_2 (Samchun Chemical, Korea), 3 wt% H_2SO_4 , and 94 wt% H_2O and heating at 80 °C for 1 h. The membrane was then heated in 200 g of deionized water at 80 °C for 1 h. The cleaned membrane was activated in a 0.5 mol/kg H_2SO_4 aqueous solution for 2 h before the fuel cell test. The activated membrane was placed between the two electrodes. The silicon gaskets were used to prevent fuel leakage between the membrane and bipolar plates. The graphite bipolar plates had serpentine flow channels that were 1 mm in width and depth. The Au-coated collectors were used to increase the electrical conductivity and the end plates were used to assemble the components. The unit cell was tightened with 20 kgf cm of clamping pressure by a torque wrench (30 QL, Tohnichi, Japan). Two K-type thermocouples (± 1.0 °C accuracy) in the end plates measured the anode and cathode temperatures.

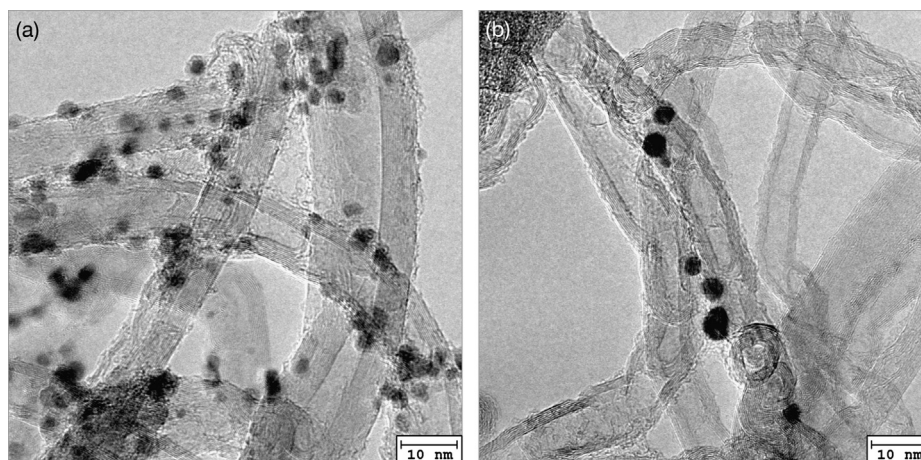


Fig. 2. TEM images of electrocatalysts: (a) Pd/MWCNTs and (b) Au/MWCNTs.

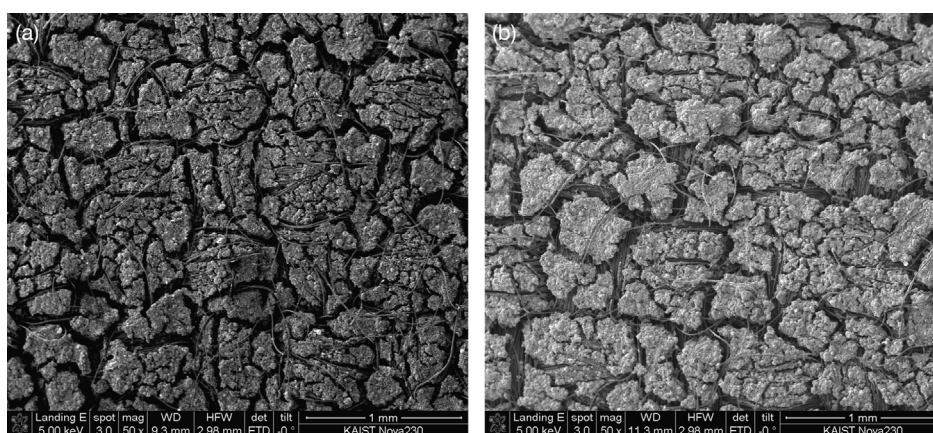


Fig. 3. Surface morphologies of the electrodes: (a) Pd/MWCNTs/carbon cloth and (b) Au/MWCNTs/carbon cloth.

2.4. Fuel cell test

A fuel cell test was conducted to evaluate the fuel cell performance. Sodium hydroxide (NaOH, Junsei Chemical, Japan) and phosphoric acid (H_3PO_4 , Samchun Chemical, Korea) were used for fuel stabilization. The fuel for the anode was composed of 5 wt% NaBH_4 , 10 wt% NaOH, and 85 wt% H_2O . The fuel for the cathode was composed of 5 wt% H_2O_2 , 5 wt% H_3PO_4 , and 90 wt% H_2O . Five hundred grams of each fuel was supplied at a rate of 10 mL/min. The fuel cell test was conducted at room temperature.

The experimental setup was the same as that used in our previous studies [52,53]. The fuels were stored in two fuel cartridges. Two power supplies (IT6720, ITECH Electronic, Taiwan) operated the two fuel pumps (Unoverse 9000, Uno International, UK) to supply the fuels from the fuel cartridges to the electrodes. The performance of the fuel cell was measured by an electronic load (3311D, Prodigit, Taiwan, $\pm 0.2\%$ accuracy). The current density of the fuel cell was adjusted from 0 to 360 mA/cm^2 in increments of 20 mA/cm^2 . The average voltage measured for 1 min was used to calculate the power density at each current density. The liquid products were stored in two product cartridges. The hydrogen and oxygen produced from the fuel decomposition were passed through H_2O and silica gel (SiO_2 , Junsei Chemical, Japan) inside flasks to remove impurities and moisture. The volume flow rates of the dehydrated hydrogen and oxygen were measured by two volume flow meters (FMA-1605A-VOL, FMA-1608A-VOL, Omega, USA, $\pm 1.0\%$ accuracy). The measured data were acquired by a data acquisition board (Personal Daq/56, Iotech, USA).

3. Results and discussion

3.1. Fuel cell test

The electrodes with electrocatalysts supported on MWCNTs were examined through various analyses. Fig. 2 shows the TEM images of the electrocatalysts. The Pd and Au catalysts are well distributed on the MWCNTs. The surface morphologies of the electrodes are illustrated in Fig. 3. Micro-cracks of the catalyst layer on the carbon cloth were produced during electrode preparation. Liquid fuel could easily diffuse from the flow channel to the carbon cloth, electrocatalysts, and membrane owing to the micro-cracks. Fig. 4 presents the compositions of the electrodes. The anode is composed of Pd (1.07 at%), C (86.65 at%), O (7.12 at%), F (3.2 at%), and S (1.96 at%), whereas the cathode is composed of Au (2.3 at%), C (86.44 at%), O (5.78 at%), F (4.04 at%), and S (1.44 at%). O, F, and S were detected owing to oxidation and the Nafion binder like previous studies [52,53]. The microstructures of the electrodes are C (002), Pd (111), Pd (200), Pd (220), Pd (311), Au (111), Au (200), Au (220), and Au (311), similar to the results of previous research [52,53].

The performance of the fuel cell was evaluated to determine the design specifications of the DBPFC system for space missions. As shown in Fig. 5(a), the open-circuit voltage and maximum power density are 1.71 V and 110.8 mW/cm^2 , respectively. The maximum power density was lower than that achieved by research groups at Ohio State University [44], Instituto Superior Técnico [47], University of Illinois [25], Harbin Engineering University [30], and Indian Institute of Science [21]. However, it was higher than that achieved

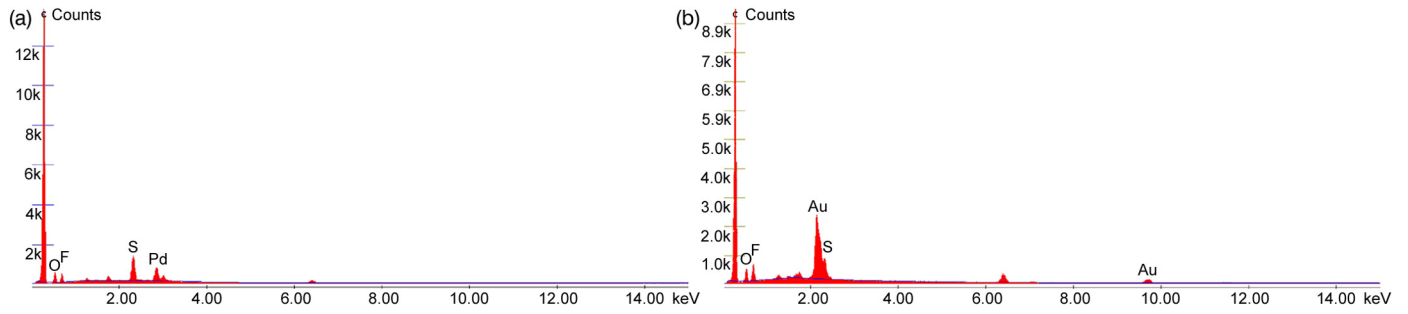


Fig. 4. Compositions of the electrodes: (a) Pd/MWCNTs/carbon cloth and (b) Au/MWCNTs/carbon cloth.

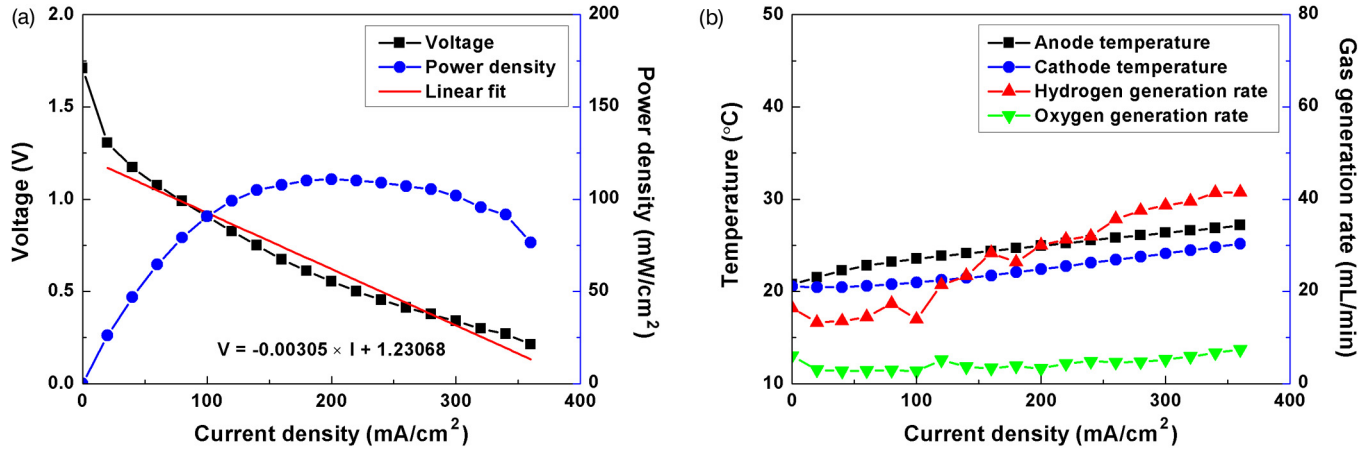


Fig. 5. Fuel cell test: (a) performance curve and (b) temperatures and gas generation rates.

by research groups at Xiangtan University [41], Taiyuan University of Technology [58], University of Southampton [23], Nanjing University [49], and Tsinghua University [43]. The voltage efficiency at the maximum power density is 18.4%. Because a relationship between the current density and voltage is required to estimate the mass and energy density of the DBPFC system, Eq. (4) was obtained from the experimental data in Fig. 5(a). The temperatures and gas generation rates of the fuel cell are presented in Fig. 5(b). The maximum power density of the fuel cell increases with an increase in current density, but the voltage efficiency of the fuel cell decreases with an increase in current density. A large amount of heat was generated at the high current density because of the low voltage efficiency. As a result, the temperatures and gas generation rates increase with an increase in current density. The amount of hydrogen produced by NaBH_4 decomposition is much larger than that of the oxygen produced by H_2O_2 decomposition. Consequently, the NaBH_4 decomposition reaction on the Pd catalyst is more sensitive than the H_2O_2 decomposition reaction on the Au catalyst.

$$V = -0.00305 \times I + 1.23068 \quad (4)$$

3.2. Effect of voltage efficiency and fuel concentrations on total mass of DBPFC system

The system masses and energy densities of the power sources are important for space missions. The effect of voltage efficiency and fuel concentrations on the total mass of the DBPFC system was investigated with the fuel cell system, which had 100 W of maximum power and 5 kWh of total energy. Because the fuel cell stack and fuels make up a substantial portion of the fuel cell system with high energy and a long operating time, the mass of other components, such as the fuel pump, fuel cartridge, and product cartridge, can be neglected. As a result, the mass of the fuel cell

stack and fuels was only calculated based on the test results in Section 3.1. The mass of the fuel cell stack was estimated from the maximum power and mass of the unit cell, as shown in Eq. (5) [68–70]. In the equation, P_{stack} is the maximum power of the fuel cell stack, $P_{\text{unit cell}}$ is the maximum power of a unit cell, $M_{\text{unit cell}}$ is the total mass of a unit cell, η_{voltage} is the voltage efficiency, and E^0 is the theoretical voltage of the DBPFC. The fuel mass was calculated using Eq. (6) [68–70]. E is the total energy of the fuel cell system, MW_{fuel} is the molecular weight of the fuel, N_{fuel} is the theoretical number of electrons generated from 1 mol of fuel, F is the Faraday constant, C_{fuel} is the fuel concentration, and η_{fuel} is the fuel utilization efficiency. The fuel utilization efficiency was assumed 100% [28]. P_{stack} , $M_{\text{unit cell}}$, E^0 , E , MW_{fuel} , N_{fuel} , F , and η_{fuel} are constants. Consequently, M_{stack} and M_{fuel} can be determined by η_{voltage} and C_{fuel} .

$$M_{\text{stack}} = \frac{P_{\text{stack}}}{P_{\text{unit cell}}} \times M_{\text{unit cell}} = \frac{-0.00305 \times P_{\text{stack}}}{\eta_{\text{voltage}} \times E^0 \times (\eta_{\text{voltage}} \times E^0 - 1.23068)} \times M_{\text{unit cell}} \quad (5)$$

$$M_{\text{fuel}} = \frac{E \times MW_{\text{fuel}}}{N_{\text{fuel}} \times \eta_{\text{voltage}} \times E^0 \times F \times C_{\text{fuel}} \times \eta_{\text{fuel}}} \quad (6)$$

Fig. 6(a) presents the effect of voltage efficiency and NaBH_4 concentration on the total mass of the DBPFC system. The H_2O_2 concentration was assumed to be 10 wt%. As the voltage efficiency increases from 5% to 35%, the system mass decreases. However, the system mass increases when the voltage efficiency is higher than 35%. This is due to the stack mass. At voltage efficiencies less than 20%, the maximum power density increases with an increase in voltage efficiency; however, when the voltage efficiency is greater than 20%, the maximum power density decreases with an increase

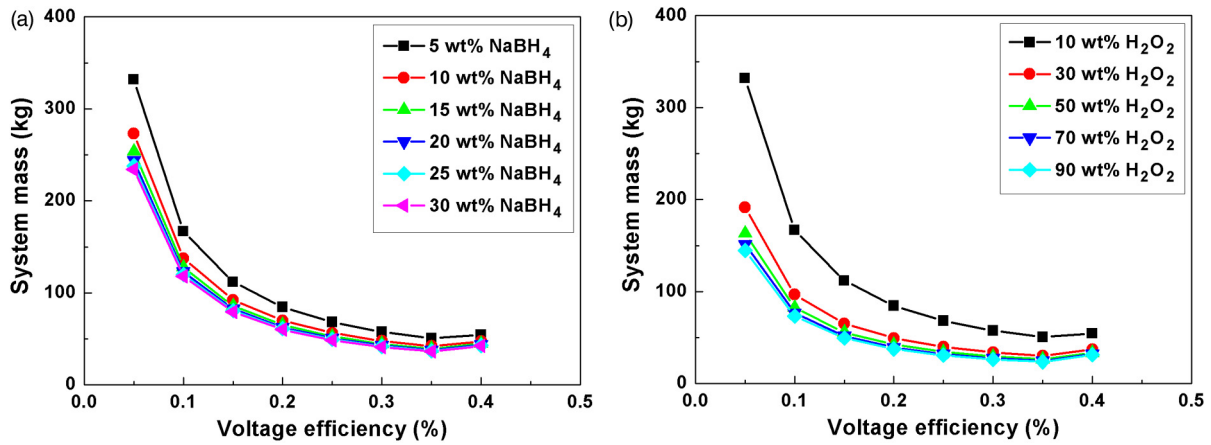


Fig. 6. Effects of voltage efficiency and fuel concentrations on total mass of DBPFC system: (a) NaBH₄ concentration and (b) H₂O₂ concentration.

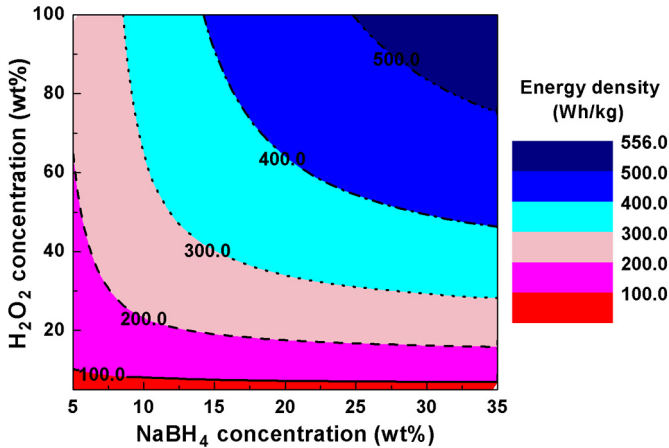


Fig. 7. Energy densities of DBPFC system at various fuel concentrations.

in voltage efficiency. As a result, the stack mass decreases and increases at 20% of the voltage efficiency. Although the fuel weight decreases with an increase in voltage efficiency, the system mass increases because of the increase of the stack mass. At constant voltage efficiency, the system mass decreases slightly as the NaBH₄ concentration increases. Fig. 6(b) shows the effect of voltage efficiency and H₂O₂ concentration on the total mass of the DBPFC system. The NaBH₄ concentration was assumed to be 5 wt%. The system mass is lowest at 35% voltage efficiency, which is the same as the result from Fig. 6(a). In addition, the system mass decreases with an increase in H₂O₂ concentration.

The system mass is lowest at 35% voltage efficiency, regardless of the NaBH₄ and H₂O₂ concentrations. Consequently, the DBPFC system should be operated at this voltage efficiency to achieve high energy density. If the DBPFC system is operated at the optimum voltage efficiency for high energy density, the system mass and energy density of the DBPFC system can be determined using only the fuel concentrations.

3.3. Estimation of the energy density of DBPFC system for space missions

Because the energy density of the DBPFC system operating at the optimum voltage efficiency can be determined by the fuel concentrations, the energy density of the DBPFC system was estimated at various fuel concentrations to determine the design specifications of the DBPFC system for space missions. Fig. 7 shows the energy density of the DBPFC system at various fuel concentrations. The H₂O₂ concentration was varied from 5 to 100 wt%, but

Table 1 Comparison of the energy densities among various power sources.

	Gravimetric energy density (Wh/kg)	Reference
DBPFC (NaBH ₄ /H ₂ O ₂)	>400 (NaBH ₄ : >20 wt%, H ₂ O ₂ : >65 wt%)	This paper
PEMFC (NH ₃ BH ₃ /O ₂)	417	[8]
PEMFC (NaBH ₄ /O ₂)	252.1	[12]
PEMFC (NaBH ₄ /O ₂)	113.8	[10]
Lithium-sulfur battery	418.5	[72]
Lithium-ion battery	285	[73]
Sodium-ion battery	130	[74]

the NaBH₄ concentration was varied from 5 to 35 wt% because of the NaBH₄ solubility in H₂O (55 g/100 g of H₂O at 25 °C) [71]. As shown in Fig. 7, the fuel concentrations should be as high as possible to achieve high energy density. If the NaBH₄ and H₂O₂ concentrations are 35 and 100 wt%, respectively, the energy density of the DBPFC system will be 554.87 Wh/kg. The energy density of the DBPFC system with a certain concentration of fuels can be determined from Fig. 7. As a result, Fig. 7 provides new base data to develop the DBPFC system for space missions.

Table 1 compares the energy densities of various power sources. When the NaBH₄ concentration is higher than 20 wt% and the H₂O₂ concentration is higher than 65 wt%, the energy density of the DBPFC system is higher than 400 Wh/kg. This value is similar to those of the PEMFC system (NH₃BH₃/O₂) and lithium-sulfur battery, and is much higher than those of the PEMFC system (NaBH₄/O₂), lithium-ion battery, and sodium-ion battery. When the NaBH₄ concentration is higher than 30 wt% and the H₂O₂ concentration is higher than 85 wt%, the energy density of the DBPFC system is higher than 500 Wh/kg. Consequently, the NaBH₄ and H₂O₂ concentrations should be increased to 20 wt% and 65 wt%, respectively. If the fuel concentrations of the DBPFC system are increased as suggested in this study, the DBPFC system can be used for space missions.

4. Conclusions

The performance of the DBPFC with electrocatalysts supported on MWNTs was evaluated to determine the design specifications of the DBPFC system for space missions. A relationship between current density and voltage was determined from the experimental data. The effect of voltage efficiency and fuel concentrations on the total mass of the DBPFC system was investigated using the relationship. The total mass of the DBPFC system was the lowest at 35% voltage efficiency, regardless of the fuel concentrations. As a result, the energy density of the DBPFC system operating at this voltage efficiency can be determined using only the fuel con-

centrations. Finally, the energy density of the DBPFC system was calculated at various fuel concentrations. The design specifications of the DBPFC system for space missions were determined based on the estimated energy density. If the NaBH_4 and H_2O_2 concentrations are increased to 20 and 65 wt%, respectively, the energy density of the DBPFC system will be higher than 400 Wh/kg and the DBPFC system can be widely used for space missions. This study provides a performance target to develop the DBPFC system for space missions.

Conflict of interest statement

There is no conflict of interest.

References

- [1] T.H. Bradley, B.A. Moffitt, D.N. Mavris, D.E. Parekh, Development and experimental characterization of a fuel cell powered aircraft, *J. Power Sources* 171 (2007) 793–801.
- [2] T.J. Leo, J.A. Durango, E. Navarro, Exergy analysis of PEM fuel cells for marine applications, *Energy* 35 (2010) 1164–1171.
- [3] S.Y. Lee, I.G. Min, H.J. Kim, S.W. Nam, J. Lee, S.J. Kim, J.H. Jang, E.A. Cho, K.H. Song, S.A. Hong, T.H. Lim, Development of a 600 W proton exchange membrane fuel cell power system for the hazardous mission robot, *J. Fuel Cell Sci. Technol.* 7 (2010) 031006.
- [4] Y. Zhang, B. Zhou, Modeling and control of a portable proton exchange membrane fuel cell–battery power system, *J. Power Sources* 196 (2011) 8413–8423.
- [5] K. Kim, T. Kim, K. Lee, S. Kwon, Fuel cell system with sodium borohydride as hydrogen source for unmanned aerial vehicles, *J. Power Sources* 196 (2011) 9069–9075.
- [6] Y. Sone, A 100-W class regenerative fuel cell system for lunar and planetary missions, *J. Power Sources* 196 (2011) 9076–9080.
- [7] T. Kim, S. Kwon, Design and development of a fuel cell-powered small unmanned aircraft, *Int. J. Hydrog. Energy* 37 (2012) 615–622.
- [8] Y. Kim, Y. Kim, S. Yeo, K. Kim, K.J.E. Koh, J.E. Seo, S.J. Shin, D.K. Choi, C.W. Yoon, S.W. Nam, Development of a continuous hydrogen generator fueled by ammonia borane for portable fuel cell applications, *J. Power Sources* 229 (2013) 170–178.
- [9] J. Lee, T. Kim, Micro space power system using MEMS fuel cell for nano-satellites, *Acta Astronaut.* 101 (2014) 165–169.
- [10] T. Kim, NaBH_4 (sodium borohydride) hydrogen generator with a volume-exchange fuel tank for small unmanned aerial vehicles powered by a PEM (proton exchange membrane) fuel cell, *Energy* 69 (2014) 721–727.
- [11] S. Sayadi, G. Tsatsaronis, C. Duell, Exergoeconomic analysis of vehicular PEM (proton exchange membrane) fuel cell systems with and without expander, *Energy* 77 (2014) 608–622.
- [12] T.H. Oh, B.G. Gang, H. Kim, S. Kwon, Sodium borohydride hydrogen generator using Co-P/Ni foam catalysts for 200 W proton exchange membrane fuel cell system, *Energy* 90 (2015) 1163–1170.
- [13] B.G. Gang, W. Jung, S. Kwon, Transient behavior of proton exchange membrane fuel cells over a cobalt–phosphorus/nickel foam catalyst with sodium borohydride, *Int. J. Hydrog. Energy* 41 (2016) 524–533.
- [14] H. Kim, T.H. Oh, S. Kwon, Simple catalyst bed sizing of a NaBH_4 hydrogen generator with fast startup for small unmanned aerial vehicles, *Int. J. Hydrog. Energy* 41 (2016) 1018–1026.
- [15] R.K. Raman, N.A. Choudhury, A.K. Shukla, A high output voltage direct borohydride fuel cell, *Electrochem. Solid-State* 7 (2004) A488–A491.
- [16] R.K. Raman, A.K. Shukla, Electro-reduction of hydrogen peroxide on iron tetramethoxy phenyl porphyrin and lead sulfate electrodes with application in direct borohydride fuel cells, *J. Appl. Electrochem.* 35 (2005) 1157–1161.
- [17] N.A. Choudhury, R.K. Raman, S. Sampath, A.K. Shukla, An alkaline direct borohydride fuel cell with hydrogen peroxide as oxidant, *J. Power Sources* 143 (2005) 1–8.
- [18] R.K. Raman, S.K. Prashant, A.K. Shukla, A 28-W portable direct borohydride–hydrogen peroxide fuel-cell stack, *J. Power Sources* 162 (2006) 1073–1076.
- [19] R.K. Raman, A.K. Shukla, A direct borohydride/hydrogen peroxide fuel cell with reduced alkali crossover, *Fuel Cells* 7 (2007) 225–231.
- [20] G. Selvarani, S.K. Prashant, A.K. Sahu, P. Sridhar, S. Pitchumani, A.K. Shukla, A direct borohydride fuel cell employing Prussian Blue as mediated electron-transfer hydrogen peroxide reduction catalyst, *J. Power Sources* 178 (2008) 86–91.
- [21] P.S. Khadke, P. Sethuraman, P. Kandasamy, S. Parthasarathi, A.K. Shukla, A self-supported direct borohydride–hydrogen peroxide fuel cell system, *Energies* 2 (2009) 190–201.
- [22] C.P. León, F.C. Walsh, A. Rose, J.B. Lakeman, D.J. Browning, R.W. Reeve, A direct borohydride–acid peroxide fuel cell, *J. Power Sources* 164 (2007) 441–448.
- [23] C.P. León, F.C. Walsh, C.J. Patrissi, M.G. Medeiros, R.R. Bessette, R.W. Reeve, J.B. Lakeman, A. Rose, D. Browning, A direct borohydride–peroxide fuel cell using a Pd/Ir alloy coated microfibrinous carbon cathode, *Electrochem. Commun.* 10 (2008) 1610–1613.
- [24] G.H. Miley, N. Luo, J. Mather, R. Burton, G. Hawkins, L. Gu, E. Byrd, R. Gimlin, P.J. Shrestha, G. Benavides, J. Laystrom, D. Carroll, Direct $\text{NaBH}_4/\text{H}_2\text{O}_2$ fuel cells, *J. Power Sources* 165 (2007) 509–516.
- [25] L. Gu, N. Luo, G.H. Miley, Cathode electrocatalyst selection and deposition for a direct borohydride/hydrogen peroxide fuel cell, *J. Power Sources* 173 (2007) 77–85.
- [26] N. Luo, G.H. Miley, J. Mather, R. Burton, G. Hawkins, E. Byrd, F. Holcomb, J. Rusek, Engineering of the bipolar stack of a direct NaBH_4 fuel cell, *J. Power Sources* 185 (2008) 356–362.
- [27] N. Luo, G.H. Miley, K.J. Kim, R. Burton, X. Huang, $\text{NaBH}_4/\text{H}_2\text{O}_2$ fuel cells for air independent power systems, *J. Power Sources* 185 (2008) 685–690.
- [28] N. Luo, G.H. Miley, R. Gimlin, R. Burton, J. Rusek, F. Holcomb, Hydrogen–peroxide-based fuel cells for space power systems, *J. Propuls. Power* 24 (2008) 583–589.
- [29] S. Lux, L. Gu, G. Kopec, R. Bernas, G. Miley, Water management issues for direct borohydride/peroxide fuel cells, *J. Fuel Cell Sci. Technol.* 7 (2010) 024501.
- [30] D. Cao, D. Chen, J. Lan, G. Wang, An alkaline direct $\text{NaBH}_4\text{--H}_2\text{O}_2$ fuel cell with high power density, *J. Power Sources* 190 (2009) 346–350.
- [31] D. Cao, Y. Gao, G. Wang, R. Miao, Y. Liu, A direct $\text{NaBH}_4\text{--H}_2\text{O}_2$ fuel cell using Ni foam supported Au nanoparticles as electrodes, *Int. J. Hydrog. Energy* 35 (2010) 807–813.
- [32] J. Wei, X. Wang, Y. Wang, J. Guo, P. He, S. Yang, N. Li, F. Pei, Y. Wang, Carbon-supported Au hollow nanospheres as anode catalysts for direct borohydride–hydrogen peroxide fuel cells, *Energy Fuels* 23 (2009) 4037–4041.
- [33] F. Pei, Y. Wang, X. Wang, P. He, Q. Chen, X. Wang, H. Wang, L. Yi, J. Guo, Performance of supported Au–Co alloy as the anode catalyst of direct borohydride–hydrogen peroxide fuel cell, *Int. J. Hydrog. Energy* 35 (2010) 8136–8142.
- [34] L. Yi, Y. Song, W. Yi, X. Wang, H. Wang, P. He, B. Hu, Carbon supported Pt hollow nanospheres as anode catalysts for direct borohydride–hydrogen peroxide fuel cells, *Int. J. Hydrog. Energy* 36 (2011) 11512–11518.
- [35] L. Yi, Y. Song, X. Liu, X. Wang, G. Zou, P. He, W. Yi, High activity of Au–Cu/C electrocatalyst as anodic catalyst for direct borohydride–hydrogen peroxide fuel cell, *Int. J. Hydrog. Energy* 36 (2011) 15775–15782.
- [36] P. He, Y. Wang, X. Wang, F. Pei, H. Wang, L. Liu, L. Yi, Investigation of carbon supported Au–Ni bimetallic nanoparticles as electrocatalyst for direct borohydride fuel cell, *J. Power Sources* 196 (2011) 1042–1047.
- [37] L. Yi, B. Hu, Y. Song, X. Wang, G. Zou, W. Yi, Studies of electrochemical performance of carbon supported Pt–Cu nanoparticles as anode catalysts for direct borohydride–hydrogen peroxide fuel cell, *J. Power Sources* 196 (2011) 9924–9930.
- [38] L. Yi, L. Liu, X. Liu, X. Wang, W. Yi, P. He, X. Wang, Carbon-supported Pt–Co nanoparticles as anode catalyst for direct borohydride–hydrogen peroxide fuel cell: electrocatalysis and fuel cell performance, *Int. J. Hydrog. Energy* 37 (2012) 12650–12658.
- [39] L. Yi, Y. Song, X. Wang, L. Yi, J. Hu, G. Su, W. Yi, H. Yan, Carbon supported palladium hollow nanospheres as anode catalysts for direct borohydride–hydrogen peroxide fuel cells, *J. Power Sources* 205 (2012) 63–70.
- [40] L. Yi, L. Liu, X. Wang, X. Liu, W. Yi, X. Wang, Carbon supported Pt–Sn nanoparticles as anode catalyst for direct borohydride–hydrogen peroxide fuel cell: electrocatalysis and fuel cell performance, *J. Power Sources* 224 (2013) 6–12.
- [41] J. Liu, L. Yi, X. Wang, Q. Zhao, Y. Zhang, J. Gao, W. Wei, Investigation of nanoporous carbon supported palladium–zinc nanocomposites as anode catalysts for direct borohydride–hydrogen peroxide fuel cell, *Int. J. Hydrog. Energy* 40 (2015) 7301–7307.
- [42] L. Yi, W. Wei, C. Zhao, L. Tian, J. Liu, X. Wang, Enhanced activity of Au–Fe/C anodic electrocatalyst for direct borohydride–hydrogen peroxide fuel cell, *J. Power Sources* 285 (2015) 325–333.
- [43] W. Haijun, W. Cheng, L. Zhixiang, M. Zongqiang, Influence of operation conditions on direct $\text{NaBH}_4/\text{H}_2\text{O}_2$ fuel cell performance, *Int. J. Hydrog. Energy* 35 (2010) 2648–2651.
- [44] J. Ma, Y. Sahai, R.G. Buchheit, Direct borohydride fuel cell using Ni-based composite anodes, *J. Power Sources* 195 (2010) 4709–4713.
- [45] J. Ma, N.A. Choudhury, Y. Sahai, R.G. Buchheit, Performance study of direct borohydride fuel cells employing polyvinyl alcohol hydrogel membrane and nickel-based anode, *Fuel Cells* 11 (2011) 603–610.
- [46] D.M.F. Santos, P.G. Saturnino, R.F.M. Lobo, C.A.C. Sequeira, Direct borohydride/peroxide fuel cells using Prussian Blue cathodes, *J. Power Sources* 208 (2012) 131–137.
- [47] B. Šljukić, J. Milikić, D.M.F. Santos, C.A.C. Sequeira, D. Macciò, A. Saccone, Electrocatalytic performance of Pt–Dy alloys for direct borohydride fuel cells, *J. Power Sources* 272 (2014) 335–343.
- [48] D.M.F. Santos, T.F.B. Gomes, B. Šljukić, N. Sousa, C.A.C. Sequeira, F.M.L. Figueiredo, Perovskite cathodes for $\text{NaBH}_4/\text{H}_2\text{O}_2$ direct fuel cells, *Electrochim. Acta* 178 (2015) 163–170.

- [49] W. Jin, J. Liu, Y. Wang, Y. Yao, J. Gu, Z. Zou, Direct $\text{NaBH}_4\text{-H}_2\text{O}_2$ fuel cell based on nanoporous gold leaves, *Int. J. Hydrog. Energy* 38 (2013) 10992–10997.
- [50] R.O. Stroman, G.S. Jackson, Modeling the performance of an ideal $\text{NaBH}_4\text{-H}_2\text{O}_2$ direct borohydride fuel cell, *J. Power Sources* 247 (2014) 756–759.
- [51] R.O. Stroman, G.S. Jackson, Y. Garsany, K. Swider-Lyons, A calibrated hydrogen-peroxide direct-borohydride fuel cell model, *J. Power Sources* 271 (2014) 421–430.
- [52] T.H. Oh, B. Jang, S. Kwon, Performance evaluation of direct borohydride–hydrogen peroxide fuel cells with electrocatalysts supported on multiwalled carbon nanotubes, *Energy* 76 (2014) 911–919.
- [53] T.H. Oh, B. Jang, S. Kwon, Electrocatalysts supported on multiwalled carbon nanotubes for direct borohydride–hydrogen peroxide fuel cell, *Int. J. Hydrog. Energy* 39 (2014) 6977–6986.
- [54] B. Jang, T.H. Oh, S. Kwon, Effect of heat treatment of electrodes on direct borohydride–hydrogen peroxide fuel cell performance, *J. Power Sources* 268 (2014) 63–68.
- [55] T.H. Oh, B. Jang, S. Kwon, Estimating the energy density of direct borohydride–hydrogen peroxide fuel cell systems for air-independent propulsion applications, *Energy* 90 (2015) 980–986.
- [56] J. Kim, B. Jang, T. Lee, S. Kwon, Lightweight magnesium bipolar plates of direct $\text{NaBH}_4/\text{H}_2\text{O}_2$ fuel cell for AIP application, *Int. J. Turbo Jet-Engines* 32 (2015) 291–298.
- [57] D. Duan, X. You, J. Liang, S. Liu, Y. Wang, Carbon supported Cu–Pd nanoparticles as anode catalyst for direct borohydride–hydrogen peroxide fuel cells, *Electrochim. Acta* 176 (2015) 1126–1135.
- [58] D. Duan, J. Liang, H. Liu, X. You, H. Wei, G. Wei, S. Liu, The effective carbon supported core–shell structure of Ni@Au catalysts for electro-oxidation of borohydride, *Int. J. Hydrog. Energy* 40 (2015) 488–500.
- [59] D. Duan, H. Liu, X. You, H. Wei, S. Liu, Anodic behavior of carbon supported Cu@Ag core–shell nanocatalysts in direct borohydride fuel cells, *J. Power Sources* 293 (2015) 292–300.
- [60] S. An, J. Jin, J. Lee, S. Jo, D. Park, S. Kwon, Chugging instability of H_2O_2 monopropellant thrusters with reactor aspect ratio and pressures, *J. Propuls. Power* 27 (2011) 422–427.
- [61] S. Jo, D. Jang, S. An, S. Kwon, Chugging instability of H_2O_2 monopropellant thrusters with catalyst reactivity and support sizes, *J. Propuls. Power* 27 (2011) 920–924.
- [62] J. Lee, S. Kwon, Evaluation of ethanol-blended hydrogen peroxide monopropellant on a 10 N class thruster, *J. Propuls. Power* 29 (2013) 1164–1170.
- [63] S. Kang, D. Lee, S. Kwon, Lanthanum doping for longevity of alumina catalyst bed in hydrogen peroxide thruster, *Aerosp. Sci. Technol.* 46 (2015) 197–203.
- [64] Y. Moon, C. Park, S. Jo, S. Kwon, Design specifications of H_2O_2 /kerosene bipropellant rocket system for space missions, *Aerosp. Sci. Technol.* 33 (2014) 118–121.
- [65] D. Jang, Y. Kwak, S. Kwon, Design and validation of a liquid film-cooled hydrogen peroxide/kerosene bipropellant thruster, *J. Propuls. Power* 31 (2015) 761–765.
- [66] H. Kang, D. Jang, S. Kwon, Demonstration of 500 N scale bipropellant thruster using non-toxic hypergolic fuel and hydrogen peroxide, *Aerosp. Sci. Technol.* 49 (2016) 209–214.
- [67] E.S. Jung, S. Kwon, Autoignitable and restartable hybrid rockets using catalytic decomposition of an oxidizer, *J. Propuls. Power* 30 (2014) 514–518.
- [68] L. James, D. Andrew, *Fuel Cell Systems Explained*, second edn., John Wiley & Sons Ltd, Chichester, 2003.
- [69] F. Barbir, *PEM Fuel Cells: Theory and Practice*, first edn., Elsevier Academic Press, New York, 2005.
- [70] R. O’Hayre, S.W. Cha, W. Colella, F.B. Prinz, *Fuel Cell Fundamentals*, second edn., John Wiley & Sons Inc., New York, 2009.
- [71] B.H. Liu, Z.P. Li, S. Suda, Solid sodium borohydride as a hydrogen source for fuel cells, *J. Alloys Compd.* 468 (2009) 493–498.
- [72] L.B. Xing, K. Xi, Q. Li, Z. Su, C. Lai, X. Zhao, R.V. Kumar, Nitrogen, sulfur-codoped graphene sponge as electroactive carbon interlayer for high-energy and -power lithium–sulfur batteries, *J. Power Sources* 303 (2016) 22–28.
- [73] C. Wang, L. Wu, H. Wang, W. Zuo, Y. Li, J. Liu, Fabrication and shell optimization of synergistic $\text{TiO}_2\text{-MoO}_3$ core–shell nanowire array anode for high energy and power density lithium–ion batteries, *Adv. Funct. Mater.* 25 (2015) 3524–3533.
- [74] L. Liang, Y. Xu, C. Wang, L. Wen, Y. Fang, Y. Mi, M. Zhou, H. Zhao, Y. Lei, Large-scale highly ordered Sb nanorod array anodes with high capacity and rate capability for sodium–ion batteries, *Energy Environ. Sci.* 8 (2015) 2954–2962.